Investigation of Fatigue Crack Initiation in Ti-6Al-4V During Tensile-Tensile Fatigue

Svetlana G. Ivanova, Ronald R. Biederman, and Richard D. Sisson Jr.

(Submitted 26 July 2001; in revised form 14 January 2002)

Fatigue crack initiation in Ti-6Al-4V has been investigated in high cycle fatigue (HCF) and low cycle fatigue (LCF) regimes at stress ratio R = 0.1 using the replication technique. In all four tested α/β microstructures, the crack was initiated by fracture of equiaxed alpha grain. Fractured alpha grains are seen on the fracture surface as flat facets with features characteristic of cleavage fracture. In the regime of low stress amplitudes and in the absence of reverse loading, cleavage fracture contributes to crack initiation and early stages of crack growth in Ti-6Al-4V. This mechanism is discussed in relation to the anomalous mean stress fatigue behavior exhibited by this alloy.

Keywords fatigue crack initiation, fatigue of Ti-6Al-4V, mean stress effects, microstructure

1. Introduction

Investigations of the early stages of fatigue in α/β Ti alloys revealed the presence of flat facets on the fracture surface, the formation of which has been explained by cleavage or quasi-cleavage of equiaxed alpha grains.[1-5] Neal and Blenkinsop[6] observed that in the high cycle fatigue (HCF) regime, internal fatigue origins were often present in Ti-6Al-4V with flat alpha facet found at the crack origin. Based on Stroh's analysis,[7] they proposed a mechanism for fatigue crack initiation by cleavage along the $(10\bar{1}7)$ plane in equiaxed alpha grain due to the restricted slip. The work of Freudenthal[8] also emphasized the fact that the pseudoelastic nature of Ti-6Al-4V leads to development of very high stress intensification at the strain incompatibilities. In the same vein, Steel and McEvily[9] suggested that the crack initiation in Ti-6Al-4V differs from that in a "plastic" material, such as copper, in that the internal stress-concentration rather than the slip-band roughening is responsible for crack initiation in the high cycle range, possibly by the cleavage cracking, as discussed by Neal and Blenkinsop.[6]

More recently, crack initiation in α/β Ti alloys has become a focus of extensive research effort to investigate anomalous mean stress sensitivity of fatigue strength of Ti-6Al-4V.[10,11] This anomalous mean stress behavior manifests itself in negative deviation from the Goodman line and is only observed in the HCF regime. Adachi and colleagues[10] explained mean stress sensitivity in Ti-6Al-4V by the presence of hard T-textured equiaxed alpha grains restricting penetration of slip and causing fatigue crack to form at the grain boundary.

As of now, the questions of whether cleavage is involved in crack initiation in Ti-6Al-4V and what is the mechanism for flat facet formation seen on the Ti-6Al-4V fracture surface are still open. The current work was aimed to further investigate fatigue crack initiation mechanisms in Ti-6Al-4V by using the replication technique to precisely determine the fatigue crack initiation site and to monitor subsequent crack growth. Equiaxed and bimodal microstructures of Ti-6Al-4V alloy investigated in this work exhibit anomalous mean stress dependence of fatigue strength, as was previously reported by Ivanova et al.[12]

2. Experimental Procedures

Microstructures investigated in this work were obtained from two different initial materials: cross-rolled bar and forged bar. Both of them were heat-treated to yield two types of microstructure: equiaxed and bimodal. All four resulting microstructures are presented in Fig. 1. The results of chemical analysis are presented in Table 1. Table 2 gives information on heat treatments and quantitative analysis of microstructures, and Fig. 2 presents corresponding constant fatigue life diagrams.[12]

Equiaxed cross-rolled and forged microstructures are very similar. Bimodal cross-rolled material has a higher percentage of alpha phase than bimodal forged due to the lower beta transus temperature for the forged material. Texture analysis showed that all materials had similar textures of B/T type[13] with no significant differences in pole intensity between cross-rolled and forged microstructures.

Fatigue bars for the replication experiment were polished and slightly etched and then they were shot-peened, excluding a small circular-shaped area to cause the crack to initiate within this area. The specimens were fatigued at $R = 0.1$ at σ_{max} = 830 MPa low cycle fatigue (LCF regime) and σ_{max} = 620 MPa (HCF regime) on an MTS servo-hydraulic testing machine at a frequency of 30 Hz. After every 10,000 cycles, the replica of the specimen surface was taken by wrapping the replicating tape around the specimen. The collected replicas were then examined by light microscopy and SEM to determine the crack initiation site. Fracture surfaces of the broken fatigue bars were also investigated by SEM.

Svetlana G. Ivanova, Ronald R. Biederman, and **Richard D. Sisson Jr.,** Materials Science and Engineering Program, Mechanical Engineering Department, Worcester Polytechnic Institute, 100 Institute Rd., Worcester, MA 01609, U.S.A. Contact e-mail: sisson@wpi.edu.

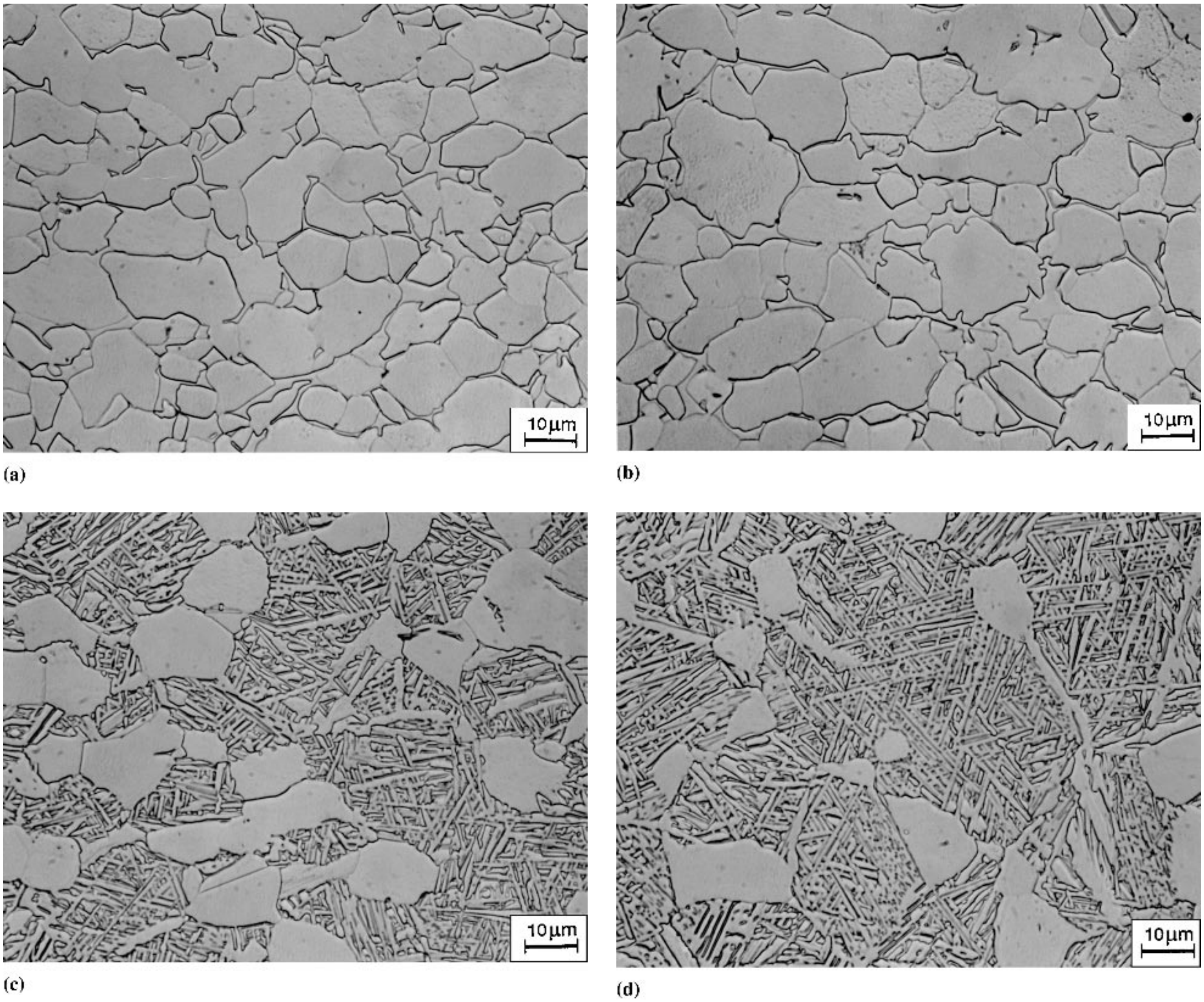

Fig. 1 Optical photomicrographs of microstructures: **(a)** equiaxed cross-rolled, **(b)** equiaxed forged, **(c)** bimodal cross-rolled, and **(d)** bimodal forged

Table 1 Results of Chemical Analysis

	Al(%)	V (%)	Fe (%)	O (%)	N (%)	H (ppm)
Cross-rolled	6.41	4.01	0.17	0.21	0.0085	68
Forged	6.07	4.16	0.15	0.18	0.0059	42
Forged rod	6.40	4.10	0.13	0.18	0.0049	38

Table 2 Heat Treatments and Microstructures

Microstructure	Heat Treatment	Volume Fraction of α Grains (%)	Average α Grain Size (μm)
Equiaxed cross-rolled	927 °C, 1 h, slow cool	85.4	6.8
Equiaxed forged	…	84.3	8.5
Bimodal cross-rolled	954 °C, 1 h, water quench	60.5	8.0
Bimodal forged	829 °C, 1 h	24.8	8.5

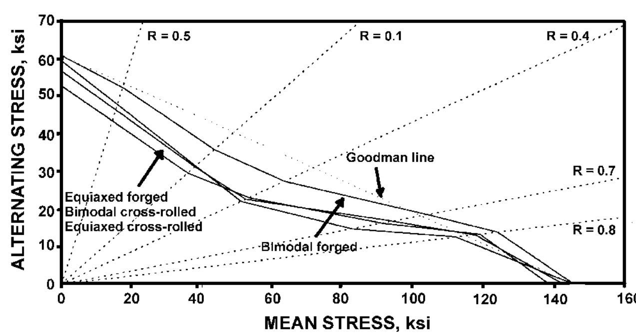

Fig. 2 Constant life diagrams at 10^7 cycles[11]

3. Results

3.1 LCF Regime

Figure 3 presents replicas of the crack nucleation site for the specimen with equiaxed forged microstructure. The crack was

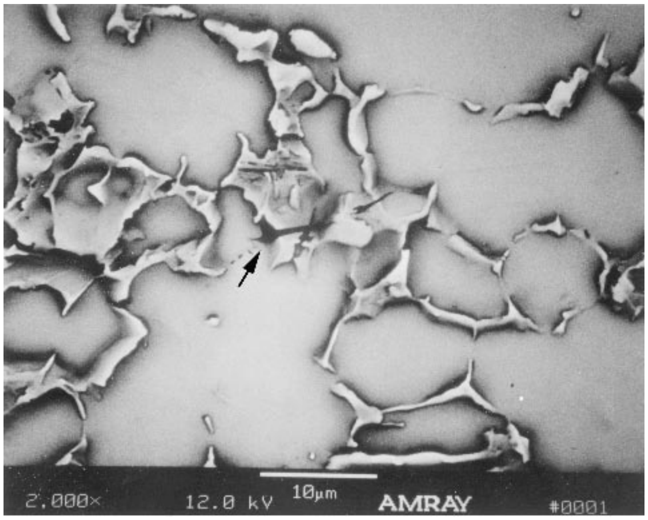

(a)

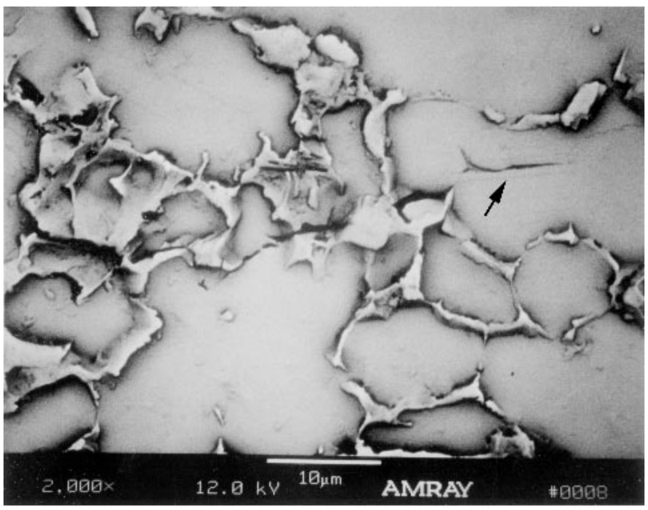

(b)

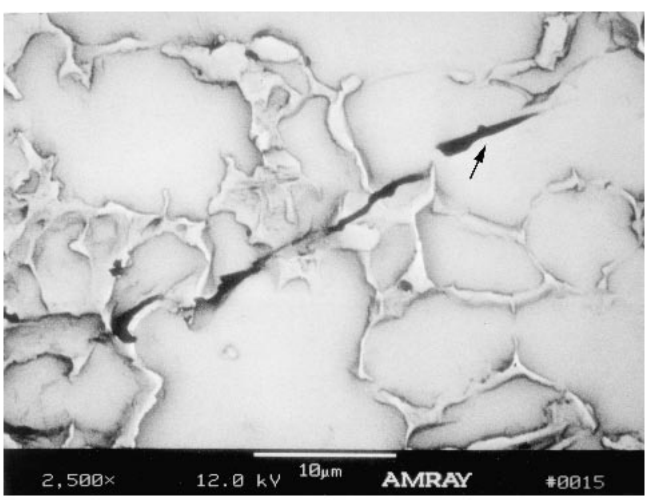

(c)

Fig. 3 Replica of crack initiation site on equiaxed forged fatigue specimen (R = 0.1, σ_{max} = 830 MPa): **(a)** after 7000 cycles, **(b)** after 9000 cycles, **(c)** after 12,000 cycles

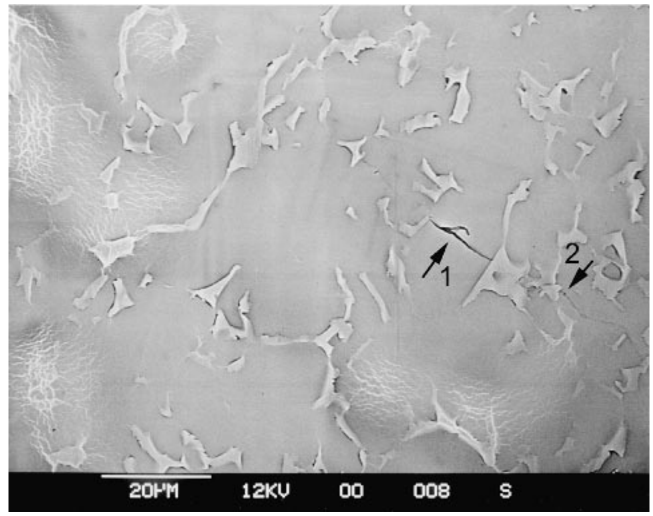

Fig. 4 Crack initiation site for equiaxed cross-rolled microstructure (R = 0.1, σ_{max} = 830 MPa, n = 15,000 cycles)

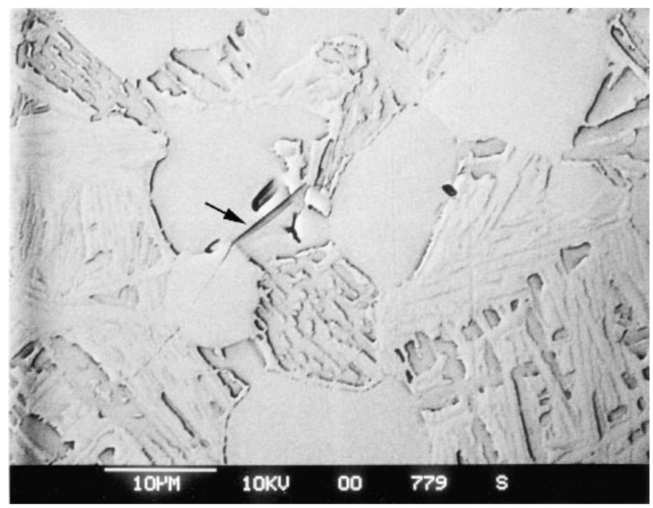

Fig. 5 Replica of the fatigue bar with bimodal forged microstructure (R = 0.1, σ_{max} = 830 MPa, n = 4000 cycles)

first detected at 7000 cycles, and it appears to have initiated at the α/β interface, as shown with an arrow on Fig. 3(a). Slip-band formation becomes evident in the neighboring alpha grain after 9000 cycles (arrow on Fig. 3b). In the initial stages, the crack propagated both through alpha grains and intergranular beta phase, as seen on Fig. 3(b). On 12,000 replica (Fig. 3c), the crack is seen to have propagated along the slip bands observed in the earlier replicas.

For equiaxed cross-rolled microstructure, the crack clearly initiated within the alpha, as shown on Fig. 4 (arrow 1). After that, the crack propagated into the next alpha grain (arrow 2), but the beta phase in-between them remained intact. It appears that the crack circumvented the beta phase beneath the surface. No signs of slip activity were observed for this microstructure.

For bimodal forged microstructure, the crack was first detected at 1000 cycles within the alpha grain. Figure 5 shows 4000 cycles replica with the arrow pointing at the crack initia-

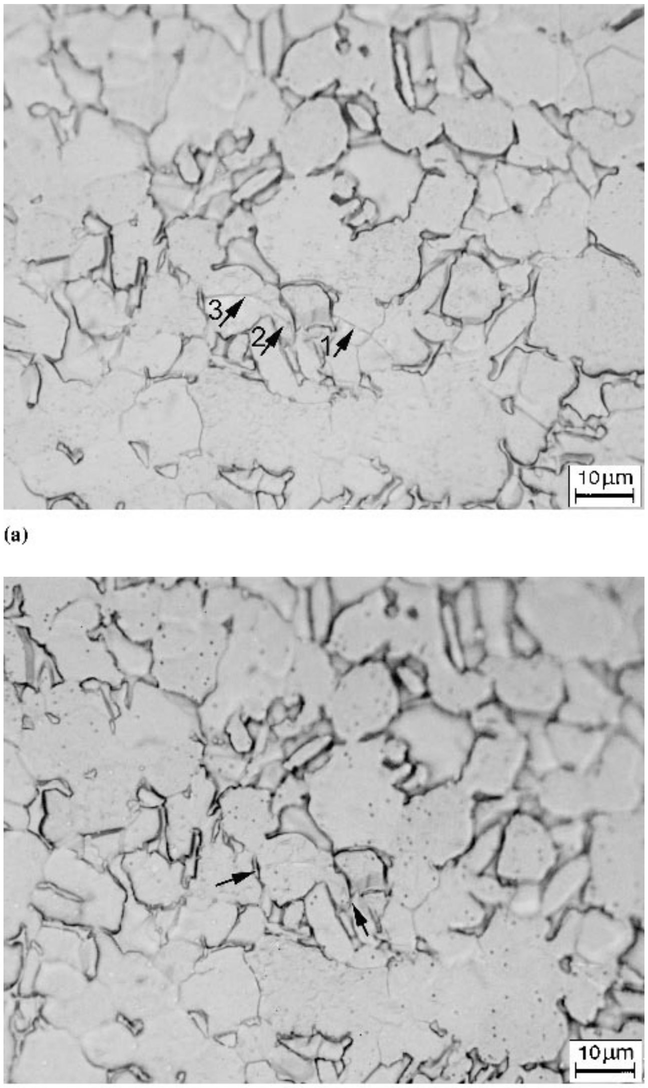

(a)

(b)

Fig. 6 Replicas of crack initiation site equiaxed forged microstructure ($R = 0.1$, $\sigma_{max} = 620$ MPa): **(a)** 270,000 cycles, **(b)** 280,000 cycles

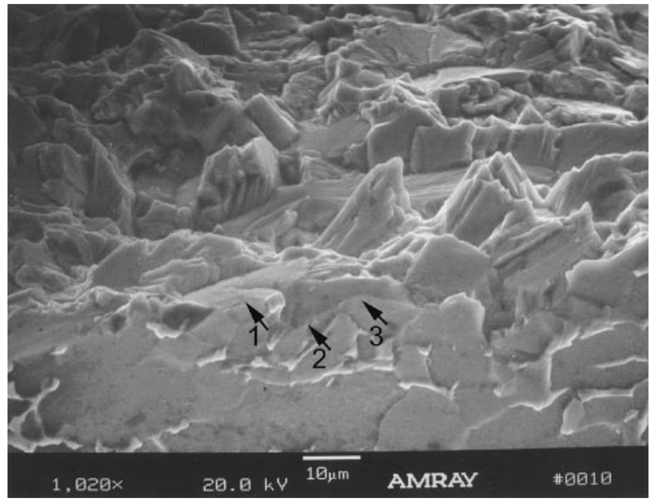

Fig. 7 Fracture surface of the replica specimen with equiaxed forged microstructure ($R = 0.1$, $\sigma_{max} = 620$ MPa)

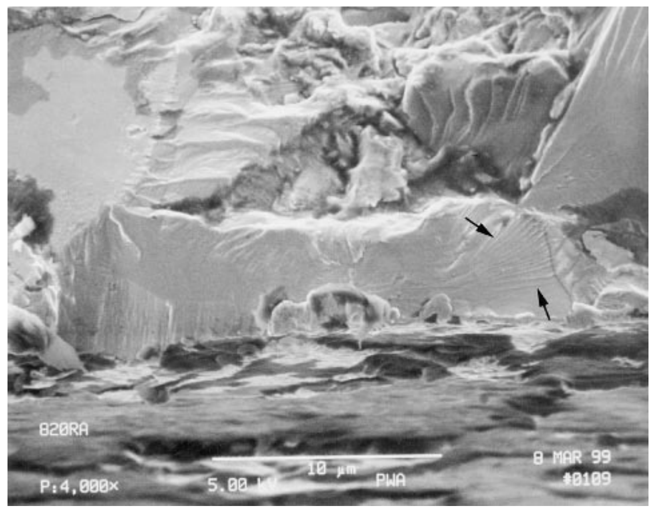

Fig. 8 Close-up via field emission microscope of the alpha grain at the fracture origin for equiaxed forged microstructure

tion site. The crack proceeded to propagate into the adjacent alpha grain and further in that direction while on the other side of the crack initiation site the crack did not start propagating until later, most likely due to the better resistance of beta-transformed phase to crack initiation and growth during the early stages of fatigue.

3.2 HCF Regime

For the equiaxed forged material, the crack initiated at 270,000 cycles in the alpha grain, starting at the α/α grain boundary (Fig. 6a). In the next 10,000 cycles, the crack extended through several alpha grains (Fig. 6b). After the specimen had been broken, its fracture surface was examined by SEM to relate microstructural features observed on the replica to the fracture surface features. Arrows 1, 2, and 3 on Fig. 6(b) and Fig. 7 correspond to the same points on the replica and the tilted fracture surface. Figure 8 presents a close-up of the fractured grain marked by arrows 2 and 3 and taken in a field emission microscope (FEM). High resolution allows us to clearly see a fan-shaped pattern on the grain surface which is characteristic of a cleavage-type fracture.[14] As was shown above on Fig. 6(a), this grain is the site where fatigue fracture initiated.

The bimodal forged microstructure showed very high resistance to crack initiation. The crack was first detected only at 1,950,000 cycles, again in the alpha grain. As seen on Fig. 9 after 1,990,000 cycles, two more alpha grains became cracked while the beta-transformed phase surrounding them was still crack-free.

Table 3 gives a summary of the replication experiments. It highlights the importance of the crack initiation step in the HCF regime, which accounts for as much as 96% of fatigue life while in the LCF regime, crack initiation takes only 25% or less of the total life.

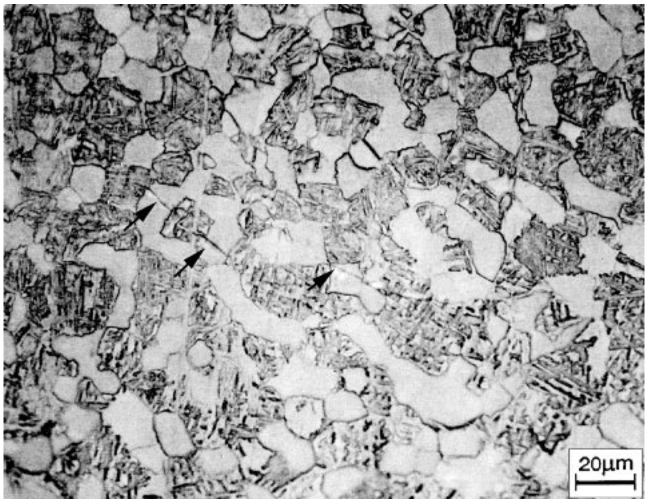

Fig. 9 Replicas of crack initiation site for material with bimodal forged microstructure ($R = 0.1$, $\sigma_{max} = 620$ MPa, $n = 1{,}990{,}000$ cycles)

Table 3 Summary of Replication Specimens

Microstructure	Fatigue Regime	Cycles to Failure	Cycles to Initiation	Percentage of Life Spent Initiating Crack
Equiaxed forged	LCF	24,000	<7000	<29%
Equiaxed cross-rolled	LCF	35,000	Unknown	—
Bimodal forged	LCF	28,000	1000	4%
Equiaxed forged	HCF	316,000	270,000	85%
Bimodal forged	HCF	2,035,000	1,950,000	96%

4. Discussion

The results of the replication experiments clearly show that the preferred fatigue crack initiation sites in Ti-6Al-4V are within the equiaxed alpha grains. Alpha grains are also more susceptible to fracture in the early stage of crack growth than the beta phase. On the fracture surface these fractured alpha grains are seen in the vicinity of the crack initiation site as cleavage-like facets with a fan-shaped pattern of fine steps characteristic of cleavage fracture. It is very likely that cleavage-type fracture contributes to the crack initiation in Ti-6Al-4V; another observation in support of this point being the absence of slip activity in the alpha phase in the HCF regime, as our replication experiment has shown. According to Adachi and Lutjering,[10] during tensile-tensile fatigue in Ti-6Al-4V, dislocations pile up at the unfavorably-oriented-for-slip T-textured alpha grains, causing stress concentration ahead of the pile-up. But, on the other hand, the orientation of these T-textured grains is such that the easy cleavage plane in Ti-6Al-4V ($10\bar{1}7$) (which is close to basal orientation) is nearly perpendicular to the loading direction, as can be seen in Fig. 10, therefore maximizing the effect of the applied tensile stress. This stress combined with tensile stress caused by dislocation pile-up in the neighboring grain can exceed fracture strength of

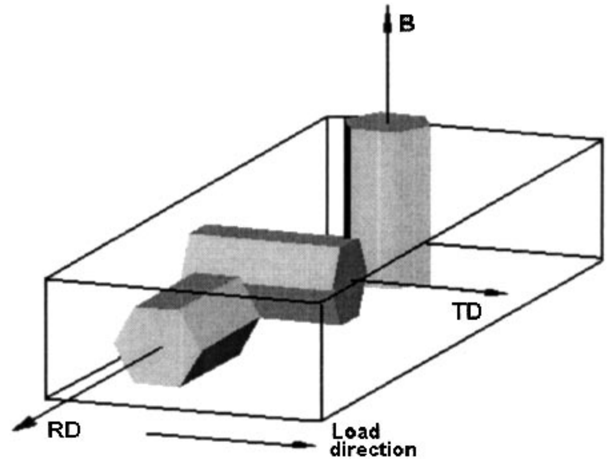

Fig. 10 Orientation of texture components in the cross-rolled material

the easy cleavage plane in this alloy, thereby initiating a fatigue crack by cleavage fracture.

Because the cleavage fracture is mostly affected by the maximum stress in a cycle, rather than by the alternating stress, Ti-6Al-4V alloy has anomalously low fatigue strength in the presence of tensile mean stresses, that is, in the loading conditions when maximum stress in a cycle is high and alternating stress is low.

5. Conclusions

Our investigation of the crack initiation process in Ti-6Al-4V indicates that in the high cycle fatigue regime, the crack initiates in the alpha phase by a cleavage fracture of T-textured alpha grains. This mechanism is likely responsible for anomalous mean stress behavior exhibited by this alloy in the high cycle fatigue regime.

Acknowledgments

We would like to thank Frederic Cohen of Pratt & Whitney for his help with the experimental part and the U.S. Air Force Office of Scientific Research for providing funding for this work (AFOSR Grant No. F49620-91-1-0143).

References

1. A.L. Dowson, C.J. Beevers, and L. Grabowski: "The Microstructural Features Associated with the Growth of Short Fatigue Cracks in a Near-Alpha Ti Alloy" in *Titanium '92. Science and Technology*, F.H. Froes and I. Caplan, ed., TMS, Warrendale, PA, 1993, pp. 1741-48.
2. R.J. Wanhill and H. Doker: "Vacuum Fatigue Fracture of Ti-6Al-4V," in *Proceedings of Third International Conference on Titanium*, Plenum Press, New York, NY, 1982, pp. 799-810.
3. P.E. Irving and C.J. Beevers: "Microstructural Influences on Fatigue Crack Growth in Ti-6Al-4V," *Mater. Sci. Eng.*, 1974, *14*, pp. 229-38.
4. K. Sadananda: "A Dislocation Model for Faceted Mode of Fatigue Crack Growth" in *Dislocation Modeling of Physical Systems*, M.F. Ashby, R. Bullough, C.S. Hartley, and J.P. Hirth, ed., Pergamon Press, New York, NY, 1981, pp. 69-73.
5. D.A. Meyn: "Analysis of Frequency and Amplitude Effects on Cor-

rosion Fatigue Crack Propagation in Ti-8Al-1Mo-1V" *Metall. Trans.*, 1971, *2*, p. 853.

6. D.F. Neal and P.A. Blenkinsop: "Internal Fatigue Origins in α-β Titanium Alloys," *Acta Metall.*, 1976, *24*, pp. 59-63.
7. A.N. Stroh: "Theory of the Fracture of Metals," *Adv. Phys.*, 1957, *6*, p. 418.
8. A.M. Freudenthal: "New Aspects of Fatigue and Fracture Mechanics," *Eng. Fract. Mech.*, 1974, *8*(6), pp. 775-93.
9. R.K. Steele and A.J. McEvily: "The High-Cycle Fatigue Behavior of Ti-6Al-4V Alloy," *Eng. Fract. Mech.*, 1976, *8*(1), pp. 31-37.
10. S. Adachi, L. Wagner, and G. Lütjering: "Influence of Mean Stress on Fatigue Strength of Ti-6Al-4V" in *Proceedings 7th International Conference on Strength of Metals and Alloys*, H.L. McQueen, J.P. Bailon, and J.I. Dickson, ed., Pergamon Press, New York, NY, 1986, p. 2117.
11. S. Adachi: *Mean Stress Dependence of Fatigue Strength in Titanium Alloys*, Ph.D. Thesis, Technischen Universitat Hamburg-Harburg, Germany, 1987.
12. S.G. Ivanova, F.S. Cohen, R.R. Biederman, and R.D. Sisson Jr.: "Role of Microstructure in the Mean Stress Dependence of Fatigue Strength in Ti-6Al-4V Alloy" in *Fatigue Behavior of Titanium Alloys*, R.R. Boyer, D. Eylon, and G. Lütjering, ed., TMS, Warrendale, PA, 1999, pp. 39-46.
13. R.I. Jaffe and G.Lütjering: "Effect of Microstructure and Loading Condition on Fatigue of Ti-6Al-4V Alloy" in *Microstructure, Fracture Toughness and Fatigue Crack Growth Rate in Titanium Alloys*, A.K. Chakrabarty and J.C. Chesnutt, ed., AIME, Warrendale, PA, 1987, p. 193.
14. G. Henry: *Fractography and Microfractography,* Vol. 5, Verlag Stahleisen, Dusseldorf, Germany, p. 445.